

A vertex reconstruction algorithm in the central detector of JUNO

Qin Liu¹ Miao He² Xuefeng Ding³ Liangjian Wen² Weidong Li² Haiping Peng¹

¹ State Key Laboratory of Particle Detection and Electronics,
and Department of modern physics, University of science and technology of China, Hefei 230026, China

² Institute of High Energy Physics, Chinese Academy of Sciences, Beijing 100049, China

³ Gran Sasso Science Institute(INFN), F. Crispi 7, LAquila, AQ 67100, Italy

Abstract: The Jiangmen Underground Neutrino Observatory(JUNO) is designed to determine neutrino mass hierarchy and precisely measure three of the neutrino oscillation parameters using reactor antineutrinos. It is also able to study many other physical phenomena, including supernova neutrinos, solar neutrinos, geo-neutrinos, atmosphere neutrinos, and so forth. The central detector of JUNO is a complex structure which contains 20,000 tons of liquid scintillator and about 18,000 20-inch photomultiplier tubes (PMTs). Currently, it is the largest liquid scintillator detector under construction. The expected energy resolution is going to reach about $3\%/\sqrt{E(MeV)}$. To meet the requirements of the experiment, an algorithm of vertex reconstruction which takes advantage of time and charge information of PMTs has been developed by deploying maximum likelihood method. The key point to the success of the reconstruction algorithm is a good understanding of the complicated optical process in the liquid scintillator.

Key words: vertex reconstruction, maximum likelihood method, liquid scintillator, PMT

1 Introduction

Jiangmen Underground Neutrino Observatory (JUNO) [1-3] is an international cooperation experiment which is designed to study neutrino physics. Its main purpose is to determine the mass hierarchy of neutrinos, which is one of the key questions of neutrino physics, and also one of the fundamental properties of neutrino. Meanwhile, a number of other frontier studies will be carried out, such as a precision measurement of the neutrino mixing matrix elements, the study of supernova neutrinos, solar neutrinos, geo-neutrinos, atmosphere neutrinos and so on.

JUNO will be built in Jiangmen city of Guangdong province, located about 700 meters underground. It is about 53 km from 10 reactors in Yangjiang and Taishan nuclear power plants. The experiment, started construction in the beginning of 2015, is expected to be in operation in 2020. The central detector of JUNO is a spherical structure which contains 20 kiloton liquid scintillator with about 18,000 20-inch PMTs around and that 25000 3-inch PMTs will be installed as well. Besides, There is an acrylic sphere with an inner diameter of 35.4 meters, serving as the container of the liquid scintillator. The sphere is immersed into a water pool and supported by a stainless steel truss, at a diameter of 40.1 m. The pure water in the pool is used to shield radioactive backgrounds from PMTs and surrounding rock and about 2000 20-inch PMTs will be installed in the water pool as cherenkov detector(see Fig. 1).

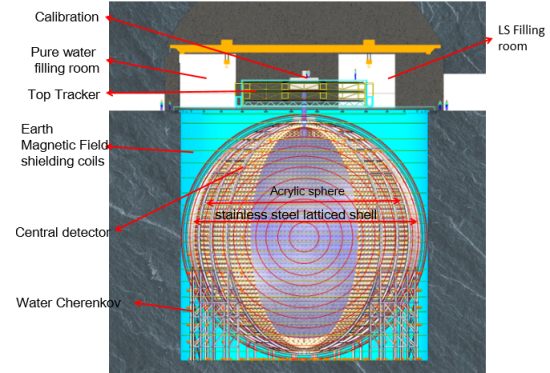


Fig. 1. detector structure.

Electron antineutrinos coming from the reactor are detected via the inverse beta decay (IBD) reaction, $\bar{\nu}_e + p \rightarrow e^+ + n$. With such a large size and high transparency of liquid scintillator, JUNO, the largest liquid scintillation detector under construction, will be able to measure the oscillated energy spectrum of neutrinos from the reactor precisely, and consequently determine the neutrino mass hierarchy. The energy resolution of the spectrum is required to be $3\%/\sqrt{E(MeV)}$.

Because of the non-uniform response of the detected number of photons over the full detector volume, the vertex of the antineutrino has to be precisely determined in the first place. Compared with current running liquid scintillation detectors[4-7], the detector volume of JUNO is much larger and the absorption or scattering of optical photons is more significant. In addition, the refractive index of the liquid scintillator is 1.49 while that of water is 1.33. This difference brings refraction and

1) E-mail: laoshe07@mail.ustc.edu.cn

total reflection which will affect the time of flight (TOF) of scintillation photons. As a result, the optical model is a challenge for JUNO and it is the critical task for the vertex reconstruction. The performances of the vertex also relies on the fluctuation of the generation of the scintillation light, as well as the timing precision of the PMT.

In this paper, we study the vertex reconstruction algorithm in the JUNO central detector. In Section 2, the principle of the vertex reconstruction algorithm is presented. Section 3 gives the detail study of the determination of TOF and Section 4 shows the distribution of the arrival time to PMTs and its impact on the vertex performance. The conclusion is given in Section 5.

2 Likelihood reconstruction algorithm

Most of the energy of reactor neutrinos is less than 10 MeV, and the spatial spread of positrons generated by IBD is a few centimeters. Compared with about 40 meters detector size, they can be safely treated as point sources. For point-like events in the liquid scintillator, a residual time is defined as the difference between the measured time and the predicted time in Eq. (1),

$$t_{i,res} = t_i - \text{tof}_i - t_0, \quad (1)$$

where t_i is the first hit time of i th PMT, tof_i is the predicted TOF of the scintillation light to the i th PMT and t_0 is the start time of an event. Apparently, tof_i depends on the event vertex and the position of the PMT. Then, the vertex $\vec{R}(x, y, z)$ and the event start time t_0 can be fitted simultaneously by maximizing an joint likelihood function

$$\mathcal{L} = \prod_i f_{res}(t_{i,res}), \quad (2)$$

where $f_{res}(t_{i,res})$ is the probability density function (PDF) of the residual time of the i th PMT. The study of TOF and PDF will be presented in detail in Sec. 3 and Sec. 4, respectively.

The likelihood fitting is usually sensitive to the initial value of the unknown parameters. The initial event start time is set as t_0 , while the initial vertex is determined by the charge center method, which is a typical way to estimate the event vertex in the liquid scintillator with less precision than using the time information. Assuming there is a point source in the liquid scintillator which emits photons isotropically, the closer the PMT to the source, the more photons will be collected and by considering the collected charge as a weight for each PMT, the source position can be estimated through formula:

$$\vec{r}_0 = \frac{\sum_i q_i \vec{r}_i}{\sum_i q_i}, \quad (3)$$

where \vec{r}_i is the position of the i th PMT and q_i is the number of photoelectrons detected in the i th PMT. Suppose the true energy deposit vertex is z_0 , one can easily calculate the vertex derived from the charge center method:

$$\begin{aligned} \langle z \rangle &= \frac{1}{4\pi} \int z d\Omega \\ &= \frac{1}{4\pi} \int_0^{2\pi} d\phi \int_0^\pi (z_0 + r \cdot \cos\theta) \sin\theta d\theta \\ &= \frac{1}{2} \int_0^\pi -(z_0 + (\sqrt{R^2 - z_0^2 \sin^2\theta} - z_0 \cos\theta) \cdot \cos\theta) d\cos\theta \\ &= \frac{1}{2} \int_{-1}^1 (z_0 + x \sqrt{R^2 - z_0^2 x^2} - z_0 x^2) dx \\ &= \frac{2}{3} z_0. \end{aligned}$$

The result is $\frac{2}{3} z_0$ and it is derived from mathematics purely, regardless of the geometry of detector and any physical processes in experiment. In algorithm, the factor is set to 1.2, which is obtained from Geant4 simulation, instead of 1.5. It is the result when considering the real optical processes during the photon propagation.

3 Time of flight in the detector

TOF is the time of flight of a scintillation photon from the time it is generated to that it is detected by a PMT. In principle, all the hit time in PMT should be used to reconstruct vertex, however, not all hits on a PMT can be identified if they are too close, especially when the deposit energy is large or the event vertex is close to the edge of the detector. Thus, the most conservative way is to use the first hit time only.

Ideally, the travel length of a photon is considered as a straight line between vertex and PMT hit. It is the most common situation for majority of the liquid detectors whose size is not large enough. In JUNO, however, there is a big difference between the refractive index of liquid scintillator and that of water, so, TOF in different materials must be calculated separately with refractive index of each material.

As is known to us all that many optical processes, such as refraction, absorption, re-emission and Rayleigh scattering [8], will change the propagation path of a scintillation photon. The larger the size of a detector, the more significant the effect will be. It turns out that the actual travel length of a photon is longer than the length of straight line assumed and cause TOF calculated smaller than the actual one.

3.1 Effective velocity

Due to the fact that scintillation photons are generated in the central detector with different wavelengths, resulting in different refractive indices and velocities,

the group velocity should be used to predict the light propagation instead of the phase velocity. According to Ref. [9], the dispersion can be parameterized by the Sellmeier equation

$$n^2(\lambda) = 1 + \frac{B}{1 - C/\lambda^2}, \quad (4)$$

where B and C are fitting parameters. The phase velocity is given by the following formula

$$V_p = \frac{\omega}{k} = \frac{c}{n}, \quad (5)$$

where c is light speed in vacuum and n is refractive index of liquid scintillator. Meanwhile, we can also calculate the group velocity according to $V_g = d\omega/dk$, if considering $\lambda = 2\pi c/\omega$ and the Sellmeier equation, we can obtain the following expression:

$$V_g = \left(\frac{c}{n}\right) \left(1 - \frac{\lambda}{n} \frac{dn}{d\lambda}\right)^{-1} = V_p \left(1 - \frac{\lambda}{n} \frac{dn}{d\lambda}\right)^{-1}. \quad (6)$$

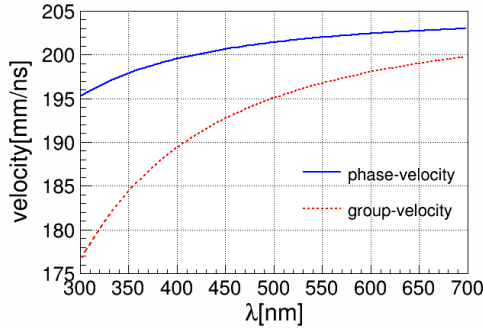


Fig. 2. phase velocity/group velocity v.s. wavelength.

Fig. 2 shows the velocity results. Combined with the luminescence spectrum of liquid scintillator, the mean phase velocity and the mean group velocity are 200.5 ± 3.0 mm/ns and 192.2 ± 3.0 mm/ns, respectively.

In fact, the effective velocity is deployed in the vertex reconstruction algorithm which is derived from the Monte Carlo simulation. The effective velocity can be obtained by the following steps: 1. Set LS luminescence time to 0 ns; 2. Put gamma source at different positions (0,0,0), (0,0,1 m), (0,0,2 m), ..., (0,0,x m) 3. Get the first hit time distribution for a certain PMT(0,0,19.5 m); 4. Calculate the effective velocity according to $v_{eff} = l/t$ by taking advantage of the peak time of the distribution. The MC simulation shows that the effective velocity is 194.8 mm/ns and seldom changes with different positions, which is very close to the mean group velocity. The difference may come from the configuration of detector. By deploying the effective velocity, the reconstructed vertex results are improved obviously.

3.2 Absorption and re-emission

Scintillation photon might be absorbed by solvent or solute of liquid scintillator during propagation and then re-emitted. Due to absorption and re-emission, the wavelength of photons will change and consequently the velocity of photons in one material will change. During this process, short wave-length photon is absorbed, afterwards long wave-length photon is emitted isotropically.

The position where re-emission happen is around energy deposit position within about several tens of centimeters. The relationship between effective refractive index and travel length of a photon is studied through MC in GEANT4[10] and it shows that the effective velocity changes less than 1% as travel distance changes which can be neglected safely.

3.3 Refraction

To correct residual time, refraction between liquid scintillation and water is considered. We have studied an ideal situation that only refraction and total reflection are considered. First, we build an optical model(Fig. 3).

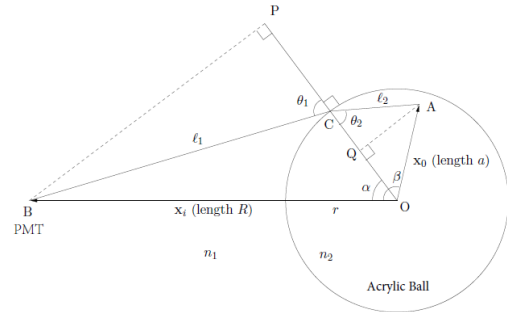


Fig. 3. Optical model used to calculate the path length of a photon from a given vertex to a specific PMT. A is the event vertex, O is the center of the detector, B is PMT's photocathode and C is the point where photon is refracted.

Then list equations below through geometry relationship and Snell's law.

$$\begin{cases} l_1 \cos \theta_1 &= R \cos \alpha \\ l_1 \sin \theta_1 &= R \sin \alpha \\ l_2 \cos \theta_2 &= r - a \cos(\beta - \alpha) \\ l_2 \sin \theta_2 &= a \sin(\beta - \alpha) \\ n_1 \sin \theta_1 &= n_2 \sin \theta_2 \end{cases}$$

The relationship between α and β is

$$1 + \left[\frac{r}{a} \csc(\beta - \alpha) - \cot(\beta - \alpha) \right]^2 = \left(\frac{n_2}{n_1} \right)^2 \left[1 + \left(\cot \alpha - \frac{r}{R} \csc \alpha \right)^2 \right] \quad (7)$$

Once α is determined, TOF can be calculated through

$$\begin{cases} l_1^2 &= R^2 + r^2 - 2Rr \cos \alpha \\ l_2^2 &= a^2 + r^2 - 2ar \cos(\beta - \alpha) \\ TOF &= (n_1 l_1 + n_2 l_2)/c. \end{cases}$$

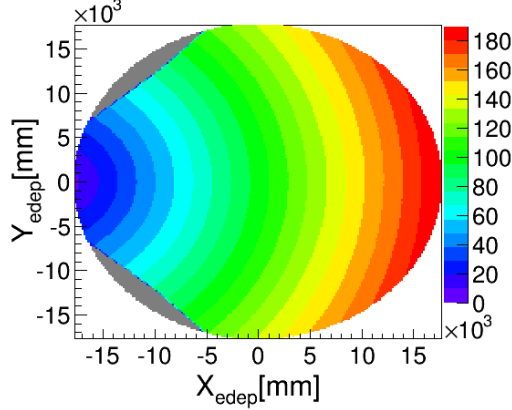


Fig. 4. TOF distribution on plane XY. The time of flight function from a test point to a PMT located at $(-R, 0, 0)$. The TOF is shown on XY-plane and the grey regions represent "dark zone". Unless it is scattered, a photon cannot travel from a point in the dark zone of a PMT to the center of that PMT's photocathode.

Fig. 4 shows the TOF distribution on plane XY. There is an obvious dark zone (grey area) due to total reflection. Fig. 5 shows the difference between straight line case and refraction case. The result demonstrates that if consider refraction, TOF almost the same when vertex is close to center of detector. However, TOF split to two when vertex is close to edge of detector. They are corresponding for near-end PMTs and far-end PMTs separately. In other words, TOF can be 8ns larger, compared with ideal situation, as propagation length of a scintillator photon becomes large.

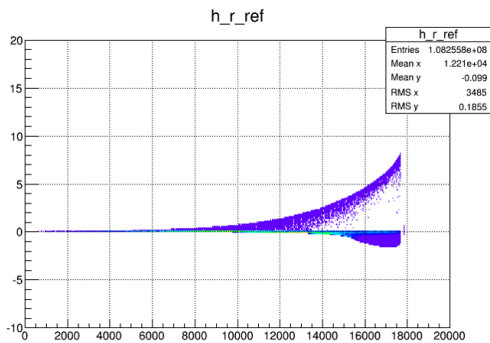


Fig. 5. TOF comparison.

3.4 Total reflection

The refractive index of liquid scintillator and water are 1.49 and 1.33 respectively. So, the critical position

where total reflection happens is about 16m according to following formula:

$$r_c = R_{LS} \times \frac{n_{water}}{n_{LS}}, \quad (8)$$

Theoretically, there will be no photon accepted in dark zone because of total refraction. In reality, however, there are still photons that can travel from a point in the dark zone of a PMT to the center of that PMT's photocathode due to Rayleigh scattering and edge effect.

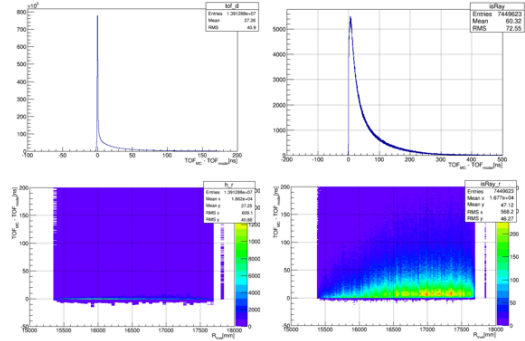


Fig. 6. TOF in dark zone comparison between MC and model. Most estimations are consistent with simulation. For Rayleigh scattering photons (second column), the bias becomes large and is broadened widely. The closer to the edge, the worsen the estimation is.

Fig. 6 shows difference of TOF between MC and predicted. As you can see, The real TOF of photon which Rayleigh scattering occurs is about 10ns larger than expected. To sum up, in dark zone of a PMT, direct photons exit as well as indirect photons which Rayleigh scattering occur. For direct photons, optical model can describe their behaviors precisely, however, the model for scattering photons still need to be further studied. We also tried to remove signals of dark zone to do reconstruction, but the result even becomes worse.

3.5 Rayleigh scattering

Rayleigh scattering can be thought as elastic scattering which means it will change only the travelling directions of photons. It will spread the time of flight of PE. The scattered light will follow the well-known angular distribution predicted by Rayleigh's theory[9], which can be characterized by the volume scattering function $\beta(\theta)$,

$$\beta(\theta) = R \left(1 + \frac{1 - \delta}{1 + \delta} \cos^2 \theta \right), \quad (9)$$

where δ is the depolarization ratio which means polarization of scattered light at 90° and R is volume scattering function at 90° , $R \equiv \beta(90^\circ)$.

However, it is pretty challenging to predict the time of flight of each PE. Currently, the strategy is set a time

window and abandon signals outside the time window. Fig. 7 shows that the pdf value is dominated by the part from -5ns to 30ns which is the range of time window. By this way, we can reduce the impact of Rayleigh scattering.

4 Probability density function

In the liquid scintillator detector, the probability density function of the arrival time of each single photon can be described as:

$$f_{res}(t) = \frac{1}{\sqrt{2\pi}\sigma} \exp\left\{-\frac{(t-t_0)^2}{2\sigma^2}\right\} \otimes \left[\frac{\omega}{\tau_1} e^{\frac{t}{\tau_1}} + \frac{1-\omega}{\tau_2} e^{\frac{t}{\tau_2}}\right]. \quad (10)$$

It is the devolution of two terms. The exponential term represents the luminescence time of the liquid scintillator where τ_1 and τ_2 correspond to the fast and slow components. The gaussian term is responsible for the systematic uncertainty of the hit time, which is dominated by the transit time spread (TTS) of PMT.

Assume a PMT collects N photons and PDF of the time of the first hit $f(t, N)$ can be derived from Eq. 11

$$f(t, N) = N f(t) \left(\int_t^{+\infty} f(x) dx \right)^{N-1}, \quad (11)$$

where $f(t)$ corresponds to PDF when PMT collects a single photon. Examples of PDF in case of different number of photons are shown in Fig. 7. Apparently, the more photons are detected, the early the first hit time is, and the precision of timing becomes higher.

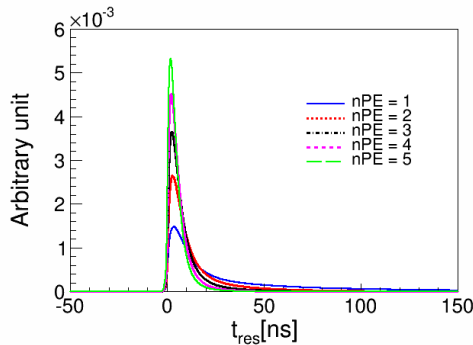


Fig. 7. PDF for different number of photons. The more PE, the sharper the PDF is. When number of PE is more than 5, the PDF are similar and obey gaussian distribution.

4.1 Number of PDF

By default, 5 PDF are deployed in reconstruction algorithm. We define a ratio: the number of PMTs that

detect photons no more than 5 to the number of all PMTs that detect photons. From Fig. 8, we can see the relationship among ratio, deposit energy and deposit vertex. As you can see that when energy becomes large or vertex get close to the edge of detector, the ratio turns to small which means more number of PDF should be considered. In reality, if one PMT receives more than 5 photons, 5-PE PDF will be deployed as well, because we found PDF is similar above 5 PE.

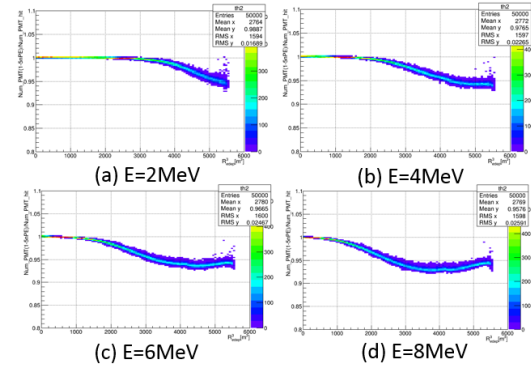


Fig. 8. Relationship among ratio, the number of PMTs that detect photons no more than 5 to the number of all PMTs that detect photons, position and energy of an event.

4.2 Difference between γ and e^+ source

Experimentally, the residual time distribution can be accessed by a particle source at the detector center. A traditional calibration source can be some γ source. However, the travel length of photon in the detector is relatively large, therefore it can influence the resulted residual hit time distribution. For comparison, we have listed the calibrated residual time distribution from MC simulation in Fig. 9.

Positron deposits energy in liquid scintillator by two steps: first, it loses energy until its kinetic energy becomes zero, then annihilates with an electron and emits a pair of gamma whose energy is 0.511 MeV. For low energy e^+ events, the source is tend to be a gamma source while for high energy event, it is more likely to be a positron source. For high energy e^+ events, γ source pdf may introduce a little bias of vertex reconstruction results. If possible, we may chose a proper source to obtain pdf. However, in calibration, positron source is not accessible.

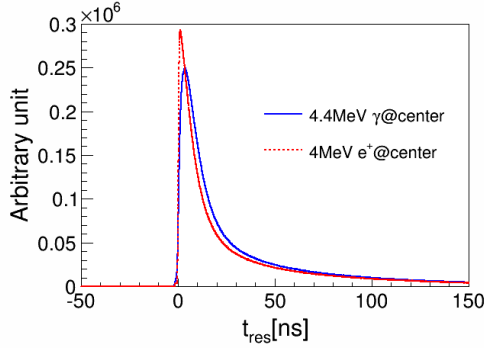


Fig. 9. Pdf comparison between 4.4 MeV γ source and 4 MeV e^+ source at detector center. Due to the fact that space dispersion effect of γ is much larger than that of e^+ , the pdf shape of e^+ is much sharper than that of γ .

4.3 PMT TTS impact on vertex reconstruction

Fig. 10 and Fig. 11 illustrate the performance of vertex reconstruction. Bias of vertex is less than 3 cm in fiducial volume (R is less than 17.2 m).

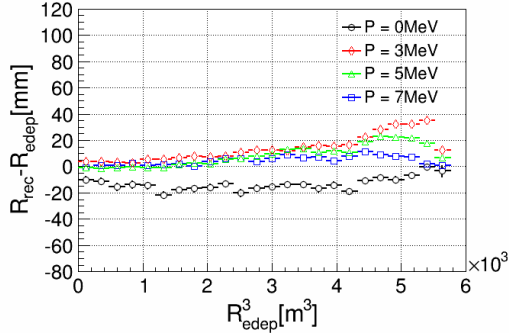


Fig. 10. Reconstructed vertex bias. By deploying the 5-pdf, considering refraction and set a time window from -5 ns to 30 ns, the bias of reconstructed vertex is less than 4 cm without any correction.

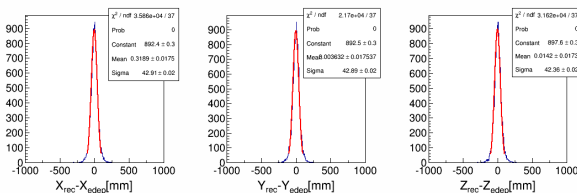


Fig. 11. Reconstructed vertex resolution of X, Y, Z direction. The mean values are consistent with MC truth and σ are similar for three directions.

Currently, the TTS of 20 inch PMT can be as large as 20 ns [11]. In other words, σ of time resolution of PMT will be 8 ns, according to the relationship $TTS = 2.354\sigma$.

Compared with liquid scintillator luminescence time, the fast component of which is 4.93 ns and the slow component is 20.6 ns, PMT TTS will dominate the uncertainty of travel time of photon-electron especially when vertex is close to PMT. Fig. 12 shows how PMT TTS influences vertex resolution. If no TTS is considered, the vertex resolution is about 7 cm@1 MeV. If TTS is about 10 ns, vertex resolution increase to 11 cm@1 MeV. In the future, 3 inch small PMT might be used to multi-purpose. Its TTS can be as good as 1ns which is much better than 20 inch PMT. The vertex resolution could improve, but how good it can reach is beyond content of this article and needs further study.

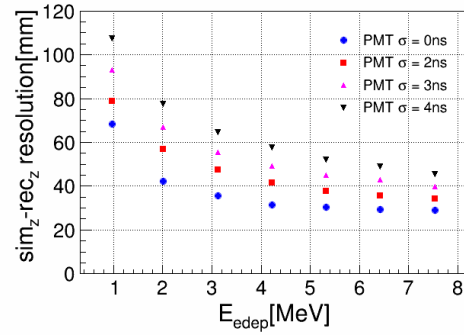


Fig. 12. PMT TTS impact on vertex resolution.

5 Conclusion

Jiangmen underground neutrino observatory (JUNO) is a multi-purpose neutrino experiment which is under construction smoothly. Its huge size and materials used in central detector makes it unique compared with other running detectors. To meet the requirement that expected energy resolution to be $3\%/\sqrt{E(\text{MeV})}$, an algorithm of vertex reconstruction has been developed. This algorithm make use of maximum likelihood method by taking advantage of time and charge information of PMTs and preliminary results about vertex has been introduced, combining the study of optical model in detector. By deploying reconstruction algorithm, the reconstructed vertex bias is within 3 cm in fiducial volume and vertex resolution is 7 cm@1 MeV if TTS is not considered.

Acknowledgements

This work is supported by National Science Foundation for Distinguished Young Scholars of China (Grant No. 11625523), National Natural Science Foundation of China (Grant No. 11575226, 11575224), and the Strategic Priority Research Program of the Chinese Academy of Sciences (Grant No. XDA10010900).

References

- 1 Djurcic, Zelimir et al. JUNO Collaboration arXiv:1508.07166
- 2 An, Fengpeng et al. JUNO Collaboration J.Phys. G43 (2016) no.3, 030401 arXiv:1507.05613
- 3 Y. F. Li, J. Cao, Y. Wang, and L. Zhan, Phys. Rev. D 88, 013008(2013).
- 4 K. Abe et al., T2K Collaboration, Phys. Rev. Lett. 107, 041801 (2011).
- 5 P. Adamson et al., MINOS Collaboration, Phys. Rev. Lett. 107, 181802(2011)
- 6 Y. Abe et al., Double Chooz Collaboration, Phys. Rev. Lett. 108, 131801(2012).
- 7 J. K. Ahn et al., RENO Collaboration, Phys. Rev. Lett. 108, 191802(2012).
- 8 15C. F. Bohren and D. R.Huffman, Absorption and Scattering of Light by Small Particle(Wiley-VCH,NewYork, 1998).
- 9 Xiang Zhou et al., Rev. Sci. Instrum. 86, 073310 (2015)
- 10 S. Agostinelli et al., Geant4 Collaboration, Nucl. Instr. And Meth. A506(2003) 250
- 11 S. Qian, "The Status of the Large Area MCP-PMT R&D in 2016, JUNO internal Note.